NF_3 and F_2 Gas Fluorination of GaN Surface and Pt/GaN Interface Analyzed by Hard X-ray Photoelectron Spectroscopy

Asahiko Matsuda[a], Takashi Teramoto[b], Takahiro Nagata[c,*], Dominic Gerlach[c,1], Peng Shen[b], Shigenori Ueda[c,d], Takako Kimura[b], Christian Dussarrat[b], and Toyohiro Chikyow[e]

[a] Materials Data Platform, National Institute for Materials Science (NIMS), 1-1 Namiki, Tsukuba, Ibaraki 305-0044, Japan

[b] K.K. Air Liquide Laboratories, 2-2 Hikarinooka, Yokosuka, Kanagawa, 239-0847, Japan

[c] Research Center for Electronic and Optical Materials, NIMS, 1-1 Namiki, Tsukuba, Ibaraki 305-0044, Japan

[d] Synchrotron X-ray Station at SPring-8, NIMS, Sayo, Hyogo 679-5148, Japan

[e] Center for Basic Research on Materials, NIMS, 1-1 Namiki, Tsukuba, Ibaraki 305-0044, Japan

* Correspondence to: NAGATA.Takahiro@nims.go.jp

[1] Current affiliation; Zernike Institute for Advanced Materials, University of Groningen Nijenborgh 4, 9747 AG Groningen, The Netherlands

ABSTRACT:

The effects of NF_3 or F_2 gas annealing on epitaxially grown GaN and its interface with sputter-deposited Pt were investigated using hard X-ray photoelectron spectroscopy. Annealing GaN and Pt/GaN samples in an NF_3 atmosphere led to the emergence of prominent F 1*s* peaks and chemically shifted Ga 2*p* peaks, indicating the efficient formation of Ga–F_x species not only in the bare GaN surface but also in the Pt/GaN interface, even when the NF_3 treatment was performed after the Pt was deposited. By contrast, F_2 annealing also led to the fluorination of the GaN surface and nonfluorination of the Pt/GaN interface. Although the plasma sputtering process removed F from the surface, band shifts were observed when the treatment conditions were varied. The findings in this study suggest that NF_3 treatment is an effective post-processing method for fluorinating GaN-based systems before or after metal deposition.

KEYWORDS: Fluorination, Surface passivation, hard X-ray photoelectron spectroscopy, Gallium nitride

INTRODUCTION

One of the issues in applying GaN in devices is its high density of vacancies and associated dangling bonds [1] The fabrication of high-performance/high-reliability GaN-based devices necessitates the development of a method to passivate such defects. In Si devices, H-based processes are typically used to passivate defects by terminating the dangling bonds with H and removing the states from within the gap [2]. However, this approach is not effective for passivating defects in GaN devices [3,4,5]. As an alternative, F has been proposed as an element that could terminate the dangling bonds. This approach has been explored for Si and Ge [6,7]. F bonds tend to be very stable because of the high electronegativity of F. In addition, the small atomic radius of F is expected to result in high diffusivity, which might enable its use in an effective post-process defect passivation methodology. Incorporating F into GaN or AlGaN/GaN devices has been explored for defect passivation or modification [8,9] as well as for modifying device characteristics such as the threshold voltage [10] The incorporation of F is usually achieved by exposure to CF_4 plasma [8,10,11], ion implantation [12,13], or, less frequently, annealing in an NF_3 atmosphere [14].These methods utilize conventional Si device process technology but have high kinetic energy during the process and require high temperature heat treatment, etc., to recover from damage. In recent years, there have also been reports of atomic layer etching of GaN surfaces by HF treatment [15]. Although F termination of the surface proceeds in this process, the discussion is about the oxidation process and its removal for the purpose of atomic layer etching, and not about fluorine termination.

In a first-principles study, Yayama *et al.* compared a nonterminated GaN (0001) surface to F- and/or H-terminated surfaces [16]. Their calculations suggested that F atoms could stably terminate dangling bonds on the GaN surface and eliminate the associated gap states. In the present paper, we examined whether this effect can be realized experimentally by treating GaN samples with F-based gases—specifically, NF_3 and F_2. In terms of elementary considerations of reaction thermodynamics, fluorination of GaN is a favorable reaction given the heats of reaction for the gas NF_3 ($-\Delta H_F$ = 125 kJ/mol), GaN (110 kJ/mol), and fully fluorinated GaF_3 (1163 kJ/mol) [17,18]. We hypothesized that F_2 gas might also be effective for this purpose given the relatively low dissociation energy of an F–F bond (159

kJ/mol [19]) compared with that of an NF_2–F bond (239 kJ/mol [20]).In addition, to inspect whether the technique is feasible as a post-process dangling-bond termination method, we prepared Pt/GaN contacts and pre-/post-annealed them in an NF_3 or F_2 atmosphere. Because our region of interest lies beneath more than several nanometers of Pt, hard X-ray photoelectron spectroscopy (HAXPES) with the ability to probe depths greater than 10 nm for Pt was employed [19,21]. The large probing depth of HAXPES enabled direct observation of the Pt/GaN interface.

EXPERIMENTAL PROCEDURES

Epitaxially grown unintentionally doped GaN (0001) films (thickness: 4–6 μm) on *c*-plane sapphire (*c*-sapphire) substrates (Powdec) were used. Samples were diced into 7 × 7 mm chips and then rinsed sequentially with acetone and ethanol. Samples were annealed at 500°C for 120 s in either an NF_3 or F_2 atmosphere under 30 kPa (hereafter "NF_3-treated" and "F_2-treated," respectively). The NF_3 and F_2 gases were diluted to 2% with N_2 gas. One group of samples did not undergo Pt deposition (hereafter "Bare-GaN" samples). Two other groups of samples had a layer of Pt deposited either after (hereafter "Post-PtGaN" samples) or before (hereafter "Pre-PtGaN" samples) the gas annealing. Pt layers were deposited to a thickness of either 5, 10, and 30 nm by DC sputtering at room temperature with Ar plasma at 1 Pa. Figure S1 shows a schematic of the sample preparation process.

HAXPES measurements were carried out at the BL15XU undulator beamline of SPring-8 with a high-resolution hemispherical electron analyzer (VG Scienta R4000). Details of the HAXPES experimental setup are described elsewhere [22,23]. The incident X-ray energy and the total energy resolution were set at 5.95 keV and 240 meV, respectively. Binding energies were calibrated from the Au $4f_{7/2}$ photoelectron peak for an Au film, which was set at the same ground level as the sample. KolXPD [24] was used for curve fitting and analysis with the Voigt function (KolXPD's implementation of a pseudo-Voigt profile [23,25]) after Shirley-type background subtraction [26]. For the Pt-deposited samples, charge correction was performed by fitting the Pt $4f_{7/2}$ peak to a Doniach–Šunjić function [27] after removing the background by the Shirley function and aligning its binding-energy peak position to 71.2 eV [28,29] The surface morphology was observed by atomic force

microscopy (AFM; Hitachi High-Technologies, AFM5000II).

RESULTS AND DISCUSSION

I. Bare samples

Figure 1 shows the surface morphologies of the NF_3-, F_2-treated, and untreated (Bare-GaN) samples. None of the samples showed indications of reactions such as etching by F-based gas plasma treatment [30] although a difference in the number of point defects was observed. The treated samples retained the atomic scale step-and-terrace structures observed in the untreated sample.

Figure 2 compares the core-level spectra of the NF_3-, F_2-treated, and untreated samples. The intensity was normalized by the peak area of the N 1*s* peaks. Both the NF_3- and F_2-treated samples showed F 1*s* peak. The area intensity in the F 1*s* peak of the F_2-treated sample is 1/30 or less than that in the spectrum of the NF_3-treated sample (Fig. 2(a)). The F 1*s* peak consists of two chemical states. Bermudez *et al*. investigated the shift of F 1*s* peaks for a reaction between XeF_2 and GaN (0001) surfaces and addressed the effects of band bending and chemical shift of Ga 3*d* peaks caused by GaF_x (x = 1, 2, 3) formation [17] Our results show characteristics qualitatively similar to Bermudez's results. To our knowledge, the literature on fluorinated GaN is insufficient to determine the extent of fluorination on the basis of chemical shift; however, according to earlier PES observations of fluorinated GaAs[31,32] and Bermudez's argument [17] the two peaks observed in our measurements may indicate any two of the species represented as GaF, GaF_2, and GaF_3. The peak shifts for GaF and GaF_2 are too similar for these species to be distinguished from each other; in addition, their peak shifts are too similar to determine if one of the species is not present as a result of instability or desorption. In addition to the results presented in the present work, a comparison with other reported results suggests that the peak located at the high-binding-energy side corresponds to GaF_3 and the peak located at the low-binding-energy side corresponds mainly to GaF [33,34] A similar tendency was confirmed in other peaks. For Ga $2p_{3/2}$ peaks (Fig. 2(b)), the peak of the untreated and F_2-treated samples exhibit symmetric profiles that can be fitted with a single Voigt-type profile. The Ga $2p_{3/2}$ and N 1*s* peaks of the NF_3-treated sample has an asymmetric shape. Asymmetry is not an intrinsic feature of a photoelectron

spectroscopy (PES) peak in GaN as verified in the untreated sample. Furthermore, all of the peaks for the NF_3-treated samples shifted toward lower binding energies. On the basis of the aforementioned assignment, these shifts indicate movement of the valence band toward the Fermi level (E_F). So, the asymmetric shape is better understood as a poorly resolved satellite caused by a chemical shift. Meanwhile, the N 1*s* peaks show slight asymmetry and unclear emergence of chemically shifted peaks for all of the gas-treated samples, as shown in Fig. 2(c), which should be originated on the surface adsorption such as the N-H and/or N-O-H. The Ga $2p_{3/2}$ peak of the NF_3-treated sample can be fitted either by three Voigt functions by considering the band bending, where the satellite peak with higher binding energy is wider than the main peak, or by three Voigt peaks of equal width, where the shifted peaks are approximately 1 and 2 eV higher in binding energy than the main peak, respectively. Considering the results of the F1*s* peak and prior literature, the main component is GaF_3. In addition, the full-width at half-maximum (FWHM) values of their Ga $2p_{3/2}$ and N 1*s* peaks increased slightly compared to the untreated sample, suggesting the defect formation.

Figure 3 shows the valence-band spectra and the region close to E_F. Two observations can be made here. One concerns the in-gap states [Fig. 3(b), the entire structure of valence band is shown in the supplementary Fig. S2]. Comparing the edges of the bands reveals that the tail toward E_F is more prominent in the spectrum of the NF_3-treated sample. These data suggest an increase of the electronic states in the gap of the NF_3-treated sample. The other observation is a shift in the binding energy. The valence-band maximum for the NF_3-treated sample was estimated to be 3.0 ±0.1 eV by linear approximation, which was shifted toward E_F by 0.2 eV compared to the untreated and F_2-treated samples, consistent with the shifts of the core-level spectra. By contrast, in the gap of the F_2-treated sample showed similar changes, but smaller than the NF_3-treated sample.

The other one concerns the shape of the valence-band spectrum corresponding to the surface termination. The shape of valence-band spectra implies a change in surface termination. GaN has a polar hexagonal structure, which is strongly related to its valence-band structure [35,36,37]. The relative intensities of the valence-band peaks at the middle and lower binding energies for the GaN film, which are respectively denoted as P_1 (~5 eV), P_2 (~8 eV), and P_3 (~10 eV) in Fig. 4(b), are characteristics of the surface termination of GaN.

Ohsawa *et al*. reported that the P_1 and P_3 are dominated by the Ga 4*s* and N 2*p* states. By contrast the P_2 is dominated by N 2*p* state [37]. For the Ga-terminated GaN, the P_1 is more intense than the P_2 at the x-ray of $h\nu = 6$ keV, whereas the P_1 of N-terminated GaN conversely shows a lower intensity than the P_2. The untreated sample shows Ga-terminated characteristics, consistent with their report [37]. Typically, metal–organic chemical vapor deposition (MOCVD)-grown GaN on a sapphire substrate has a Ga-terminated surface[38] Obtaining an N-terminated surface requires additional intermediate treatments or the incorporation of a buffer layer. By contrast, the intensity of the P_1 and P_3 of the NF_3-treated samples decreases and shows a similar intensity as the P_2. As shown in Fig. 3(b), in addition to the P_1 reduction, the peak intensity around 10 eV corresponding to the Ga 4*s* and N 2*p* states relatively decreased. Note that the shape of valence-band spectra of the F_2-treated sample showed no clear change compared to the untreated sample. These reductions in peak intensity suggested the modification of the surface termination.

By combining the results of core-level spectra as shown in Fig. 2, we consider the fluorination to proceed as follows. The Ga-terminated surface ideally has dangling bonds [39]. The NF_3 or F_2 treatment acts upon the bonds, terminating them with F and resulting in a GaF_3 structure. Other bonding states may exist, such as F as an interstitial caused by the defects in GaN or surface oxidization such as Ga–O–F. Possible defects include through-dislocation structures, as observed by AFM (Fig. 1), and irregular structures resulting from unintentional surface oxidation. We have established that the NF_3 treatment terminates GaN with F to incorporate structures such as GaF_x, and the shift of E_F to the in-gap state suggesting the depletion of electrons at the surface due to this termination process were confirmed as a peak shift in the core-level spectra of the NF_3-treated samples, which is consistent with the effects suggested by first-principles calculations [16]. However, these results also indicate that the introduction of F, in addition to passivating and removing dangling bonds, increased the in-gap states associated with the nitrogen defects identified in Figure 3(b). Notably, however, the calculations only dealt with limited models in which the GaN crystal was nearly ideal and the dangling bonds were on the surface pointing toward the vacuum. Also, the emergence of multiple shifted peaks in the Ga 2p peaks indicates the presence of multiple chemical states of Ga, GaF_x (x = 1, 2, 3), which is not addressed in the calculations. A more

appropriate comparison might be with calculations that account for defects found in GaN bulk, such as a N vacancies, where the dangling bonds on Ga are terminated as Ga–F bonds.

II. Pt-deposited GaN samples

Figure 4 shows the core-level spectra in post-PtGaN samples with 10 nm-thick Pt layers. The emergence of an F 1s peak is observed for the NF_3-treated sample but not for the F_2-treated sample [Fig. 4(a)]. The NF_3-treated sample also indicates the emergence of additional shifted Ga 2*p* peaks at the higher binding energies of 1121.7, 1120.0, and 1119.8 eV compared to the primary peak at 1118.8 eV [Fig. 4(b)], which are also seen for Bare-GaN. The shifted peaks are much more prominent in the Ga 2*p* spectrum of Post-PtGaN than in that of Bare-GaN (compare the Ga 2*p* spectrum for the NF_3-treated bare sample in Fig. 2 with the corresponding spectrum for Post-PtGaN in Fig. 4). Meanwhile, the N 1*s* peak of the NF_3-treated sample shows a similar chemical shift to the Ga 2*p* peak, but slightly asymmetric as same as the bare-GaN. These results imply that F preferentially bonds with metals and/or defects, not N. Apart from the chemically shifted peaks, we note that the N 1s peak and the primary Ga 2*p* peak in the spectra of the NF_3-treated sample both shifted 0.5 eV toward higher binding energies in comparison with the corresponding peaks in the spectra of the other samples. These shifts should be interpreted in terms of E_F shifting, which coincides with the generation of gap states that act like donors at the interface. The detailed investigation was performed on the NF_3-treated Post-PtGaN samples.

Figure 5 shows the core-level spectra for the NF_3-treated Post-PtGaN samples with different Pt film thicknesses. In particular, the intensity of the highest binding energy side of the Pt 4f spectrum is enhanced in the sample with a 5 nm thick Pt film compared to the samples with 10 nm and 30 nm thicknesses [Fig. 5(a)]. This intensity increase is also not observed in the spectrum of the sample with a 5 nm-thick untreated Pt film. By contrast, for the Ga 2*p* and F 1*s* peaks of the 5 and 10 nm-thick Pt samples, peaks corresponding to fluorination were observed. In the F 1*s* peaks of the 5nm- and 10 nm-thick Pt -Post-PtGaN, peaks originating from GaF_3 and GaF_x (x=1 or 2) were observed [Fig. 5(b)], which showed the Pt-thickness dependence of the intensity ratio. At the 10 nm-thick Pt-Post-PtGaN, the intensity of GaF_3 is greater than that of GaF_x. Meanwhile, in the Ga 2p peak, the peak around

1119.5 eV was pronounced in addition to GaF_3 and GaF_x, as shown in Fig. 5(c). There are two possible explanations for these changes of peaks. One is the probing depth of our HAXPES measurement. For Pt, the inelastic mean free path [40] (IMFP) of Pt $4f_{7/2}$ for HAXPES is 4.68 nm, and the probing depth is approximately 15 nm (probing depth: 3 × IMFP [21]) below the surface in our experimental setup. Measurements of samples with a thinner Pt layer or no Pt layer resulted in the observation of more unfluorinated GaN layer beneath the fluorinated layer than the thick Pt layer; by contrast, observations through a thicker Pt layer resulted in the detection of fewer deeper unfluorinated GaN and in a higher relative percentage of fluorinated GaN closer to the interface. The second explanation is the chemical reaction of Pt by the fluorination. The NF_3 treatment enhances this fluorination or oxidation of Pt, possibly because of the catalytic reaction on Pt. Grabau *et al.* suggested that the Pt-Ga alloy system enhance the catalytic reactivity [41]. Naturally, oxidation due to atmospheric exposure and catalytic reaction occurs and the increase in peak intensity in the higher-binding-energy side of the spectrum based on Pt $4f_{7/2}$ in the Pt metal of the NF_3-treated Post-PtGaN is attributable to the surface, interface defects and its oxidation. Oxidization effects were also confirmed in the O 1*s* peaks [Fig. 5(d)]. The spectrum of the 5 nm-thick Pt sample showed relatively higher intensity. This oxidized region is not only Pt-O_x but also fluorinated Ga, and mainly a defect structure, which is thought to trap electrons and shift the HAXPES peak position to the high binding energy side away from E_F. This is confirmed by the fact that the O 1*s* peak for the 5 nm-thick Pt sample is shifted to the higher binding energy side. From the above, it is inferred that the additional peak in the Ga 2*p* is due to the binding state of oxidized GaF_x containing Pt. Although a difference exists for reactions between fluorination and oxidization, the change is comparable to the effect of untreated interface defects. As a reference experiment, electrical measurements on NF_3-treated and untreated samples were performed on a simple vertical device structure using a single crystal GaN substrate (Supplementary Fig. S3). The Fermi level shift obtained by HAXPES suggests a decrease in the Schottky barrier, however due to the interfacial oxidation, the ideal factor seems to have increased, while the effective Schottky barrier increased due to the trapping effect, so it will be necessary to control the effect of interfacial oxidation to maximize the fluorination effect.

Meanwhile, no F 1*s* signal was detected in the sample with a 30 nm thick Pt layer [Fig. 5(d)], indicating that no F atoms remain in the Pt layer itself. Furthermore, although it is possible that the GaN is fluorinated as shown by the increase in the FWHM of Ga $2p_{3/2}$, the underlying GaN is mostly beyond the probing depth of the HAXPES measurement, and the F 1*s* peak was not clearly observed. These results suggest that defects in the Pt layer are reduced and the Pt layer itself is not fluorinated. However, electrical measurements suggest that fluorine gas diffuses from the grain boundary to the interface and reacts with it, since there is a change in the Schottky barrier after post-annealing. The fluorination process may thought to be important in the vicinity of Ga. For example, a catalytic effect is expected at the Pt/GaO_x interface and NO desorption and reaction are induced. In addition, the formation of PtO_2 is promoted, although at a high temperature compared to the present experiment[42,43]. In any case, the changes in the Ga 2*p* peaks and the emergence of the F 1*s* peak clearly contrast the capabilities of the two gases: NF_3 seems to cause the Ga and F to bond, while F_2 seems to have no discernible effect, as also observed in Fig. 4.

The Pre-PtGaN samples did not show any fluorination observed for the Post-PtGaN samples, as shown in Fig. 6. The F 1*s* peak did not emerge, and the Ga 2*p* peak remained as a single symmetrical peak for the 10 nm-thick PtPre-PtGaN. Pre-PtGaN samples were subjected to gas treatment first; at this point, they were identical to the bare samples. However, the subsequent Pt sputtering deposition process apparently removes any surface modifications caused by the treatment. The highly fluorinated GaN layer might have been etched away during the sputter deposition process. These results suggest that, contrary to expectations, NF_3 treatment was effective when the gas was used for post-process treatment, whereas F_2 did not cause any fluorination in GaN.

CONCLUSION

We investigated the effects of NF_3 or F_2 gas treatment on epitaxially grown GaN and found that NF_3 is effective in fluorinating its surface, giving rise to a prominent F peak and chemically shifted Ga peaks in the corresponding HAXPES spectra, indicating the formation of GaF_x (x = 1, 2, 3) species. The effects of NF_3 treatment are observed not only in bare GaN samples but also in Pt/GaN samples treated with NF_3 after Pt deposition; however, they are

not observed for Pt/GaN samples treated with NF_3 before Pt deposition (Supplementary Fig. S4). Although our initial motivation was related to post-process passivation of defects by F-termination, our results show that fluorination may actually lead to gap states in some cases. However, the process of incorporating F into GaN has several other applications by itself, including modification of device characteristics such as the threshold voltage. The findings in the present study suggest that NF_3 treatment is an effective post-process method for fluorinating GaN-based systems after metal deposition. Moreover, compared with other fluorination methods such as exposure to CF_4 plasma, the proposed method fluorinates the GaN or its metal interface without subjecting the surface to high-energy incident ions and can therefore be considered a viable low-damage process.

ACKNOWLEDGMENTS

We are grateful to HiSOR, Hiroshima University, and JAEA/SPring-8 for the development of HAXPES at BL15XU of SPring-8. The HAXPES measurements were performed under approval of the NIMS Synchrotron X-ray Station (proposal Nos. 2016A4600, 2016B4601, 2016B4602, and 2017A4604). This work was supported in part by JSPS KAKENHI Grant No. 20H02188.

Figure Captions

Figure 1. AFM images of untreated, NF_3-treated, and F_2-treated Bare-GaN.

Figure 2. (a) F 1*s*, (b) Ga $2p_{3/2}$, and (c) N 1*s* core-level spectra for untreated, NF_3-treated, and F_2-treated Bare-GaN. The solid lines are the experimental points. The dashed lines are the Voigt profiles, and the red dots are their sum. Other Ga lines such as the $2p_{1/2}$ and 3*d* (not shown) showed similar profiles.

Figure 3. (a) Valence-band spectra near the Fermi level (E_F, 0 eV) for untreated, NF_3-treated, and F_2-treated Bare-GaN. (b) Valence-region spectra for untreated and NF_3-treated Bare-GaN. The spectrum of NF_3-treated Bare-GaN is shown shifted by -0.2 eV for shape comparison.

Figure 4. (a) F 1*s*, (b) Ga $2p_{3/2}$, and (c) N 1*s* core-level spectra for Post-Pt/GaN with 10 nm-thick Pt layer. The solid lines are the experimental points, the dashed lines are the Voigt profiles, and the red dots are their sum. Other Ga lines such as $2p_{1/2}$ and 3*d* showed similar profiles. The differences in the signal-to-noise ratios are due to different numbers of scans.

Figure 5. (a) Pt 4*f*, (b) F 1*s*, and (c) Ga $2p_{3/2}$ core-level spectra of NF_3-treated Pt/GaN with 5, 10, and 30 nm-thick Pt layer. (a) Pt 4*f* core-level spectra of untreated samples with 5 and 10 nm-thick Pt layer are also shown as references. The solid and dashed lines correspond to NF_3 gas-treated and untreated samples, respectively. (d) O 1*s* and Pt $4p_{3/2}$ core-level spectra for NF_3-treated Pt/GaN with 5, 10, and 30 nm-thick Pt layer.

Figure 6. (a) F 1*s*, (b) Ga $2p_{3/2}$, and (c) N 1*s* core-level spectra for Pre-Pt/GaN with 10 nm-thick Pt layer and untreated samples.

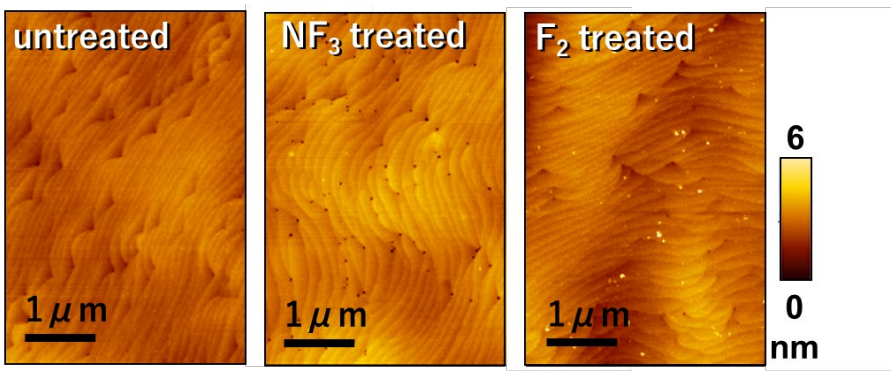

Figure 1. Matsuda *et al.*

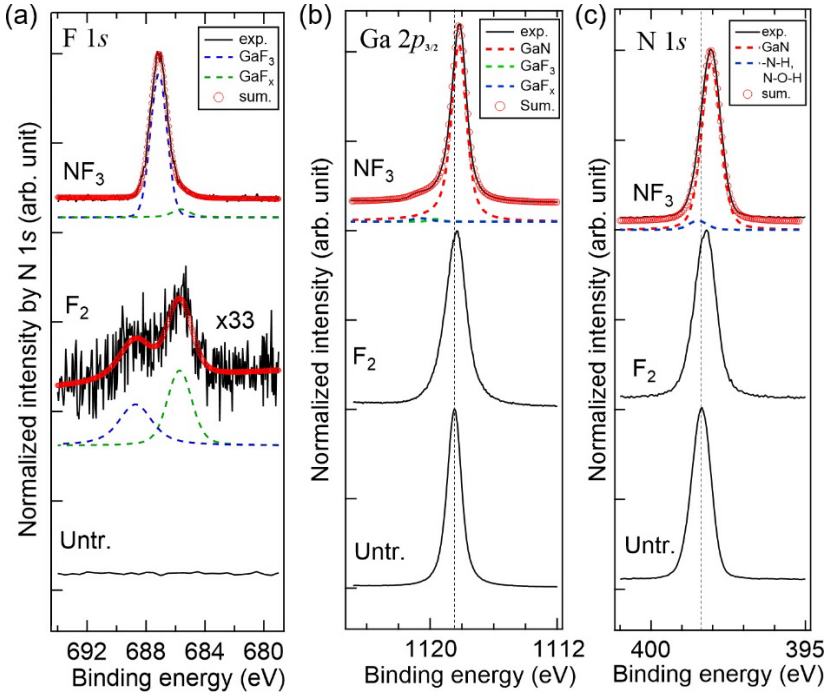

Figure 2. Matsuda *et al.*

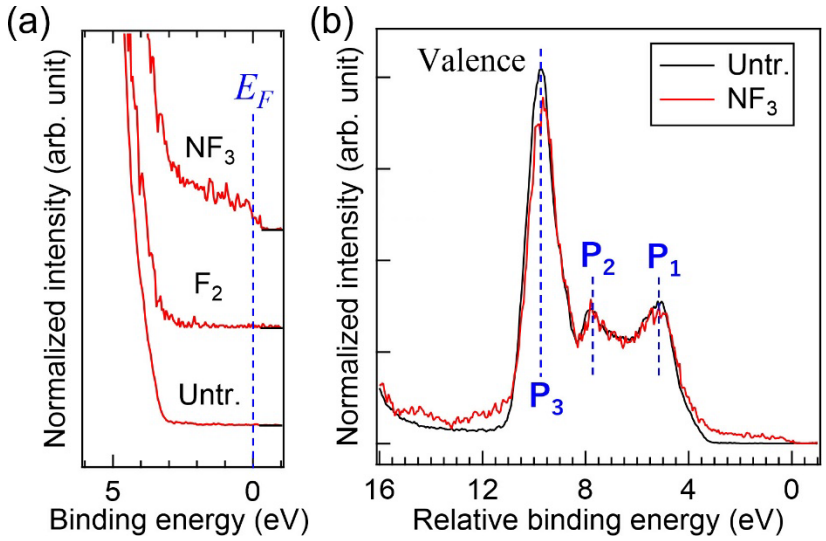

Figure 3. Matsuda *et al.*

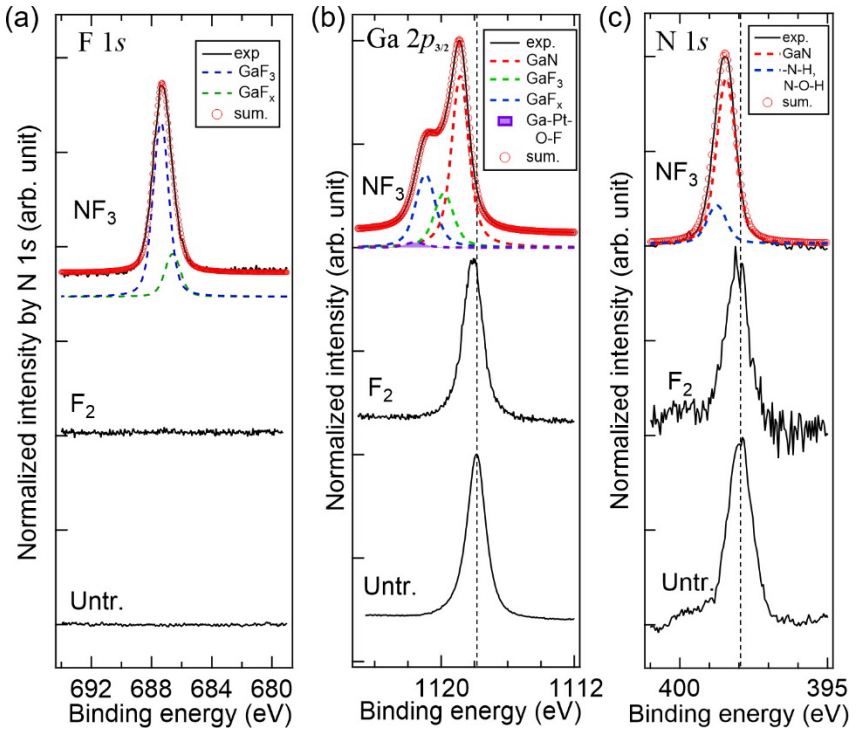

Figure 4. Matsuda *et al.*

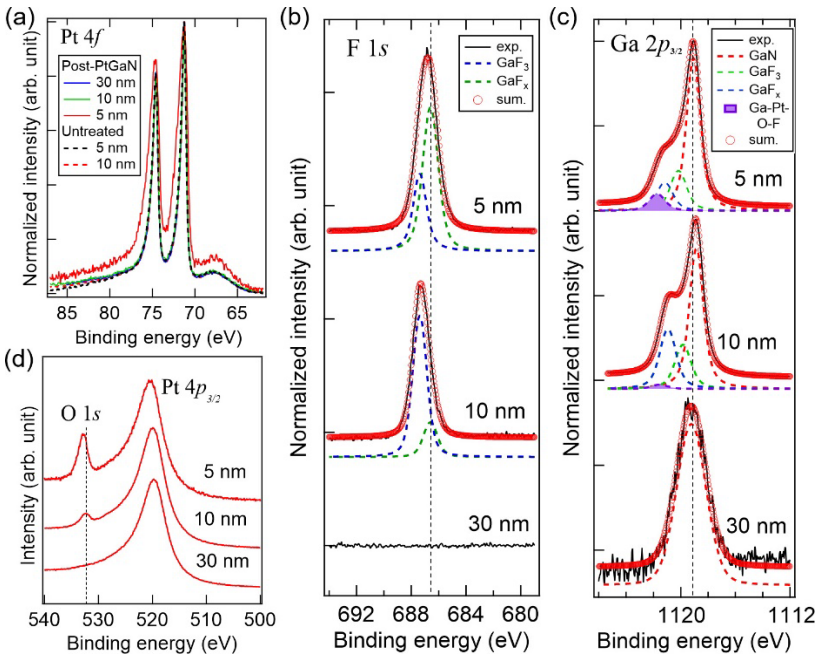

Figure 5. Matsuda *et al.*

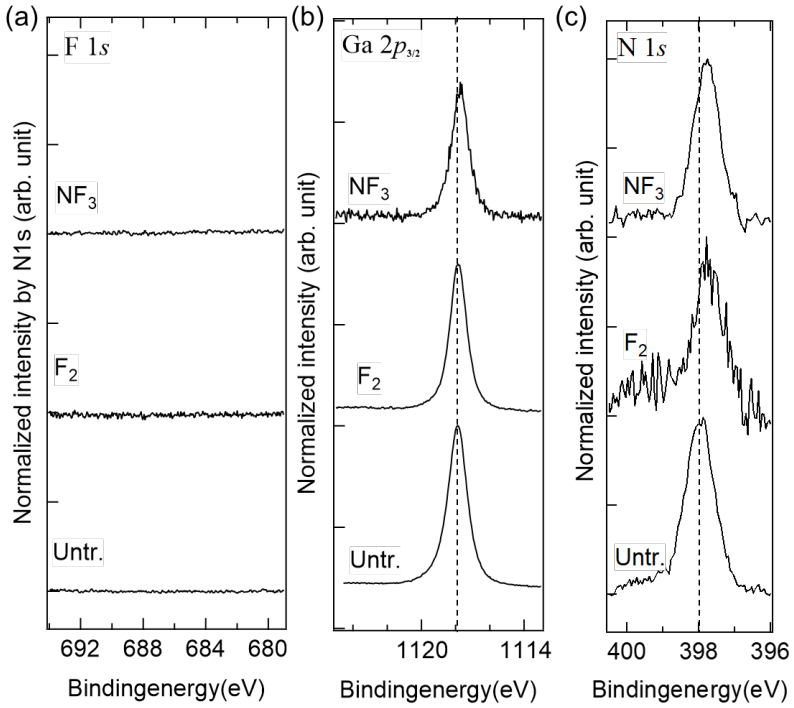

Figure 6. Matsuda *et al.*

REFERENCES

[1] S.J. Pearton, J. C. Zolper, R. J. Shul, F. Ren, GaN: Processing, defects, and devices. J. Appl. Phys. 86 (1999) 1.

[2] C.G. Van de Walle, Energies of various configurations of hydrogen in silicon. Phys. Rev. B, 49 (1994) 4579.

[3] C.G. Van de Walle, Interactions of hydrogen with native defects in GaN. Phys. Rev. B, 56 (1997) R10020.

[4] A. Hierro, S.A. Ringel, M. Hansen, J.S. Speck, U.K. Mishra, S.P. DenBaars, Hydrogen passivation of deep levels in n–GaN. Appl. Phys. Lett. 77 (2000) 1499.

[5] B. Szûcs, A. Gali, Z. Hajnal, P. Deák, C.G. Van de Walle, Physics and chemistry of hydrogen in the vacancies of semiconductors. Phys. Rev. B, 68 (2003) 085202.

[6] Pi, X. D.; Burrows, C.P.; Coleman, P.G. Fluorine in Silicon: Diffusion, Trapping, and Precipitation. Phys. Rev. Lett. 2003, 90, 155901.

[7] Jung, W.-S.; Park, J.-H.; Nainani, A.; Nam, D.; Saraswat, K.C. Fluorine passivation of vacancy defects in bulk germanium for Ge metal-oxide-semiconductor field-effect transistor application. Appl. Phys. Lett. 2012, 101, 072104.

[8] H. Chen, C.-H. Kao, Y.-C. Chen, H.-K. Lo, Y.-M. Yeh, T.-C. Lu, H.-M. Huang, C.-S. Lai, Passivation of yellow luminescence defects in GaN film by annealing and CF_4 plasma treatment. J. Optoelectron. Adv. Mater. 13 (2011) 973.

[9] M. Reiner, P. Lagger, G. Prechtl, P. Steinschifter, R. Pietschnig, D. Pogany, C. Ostermaier, Modification of "native" surface donor states in AlGaN/GaN MIS-HEMTs by fluorination: Perspective for defect engineering. in 2015 IEEE Int. Electron Devices Meet. IEDM (2015) 35.5.1.

[10] Y. Cai, Y. Zhou, K.M. Lau, K.J. Chen, Control of threshold voltage of AlGaN/GaN HEMTs by fluoride-based plasma treatment: from depletion mode to enhancement mode. IEEE Trans. Electron Devices, 53 (2006) 2207.

[11] S. Huang, H. Chen, K.J. Chen, Effects of the fluorine plasma treatment on the surface

potential and Schottky barrier height of $Al_xGa_{1-x}N$/GaN heterostructures. Appl. Phys. Lett. 96 (2010) 233510.

[12] M.J. Wang, L. Yuan, C.C. Cheng, C.D. Beling, K.J. Chen, Defect formation and annealing behaviors of fluorine-implanted GaN layers revealed by positron annihilation spectroscopy. Appl. Phys. Lett. 94 (2009) 061910.

[13] M.J. Wang, L. Yuan, K.J. Chen, F.J. Xu, B. Shen, Diffusion mechanism and the thermal stability of fluorine ions in GaN after ion implantation. J. Appl. Phys. 105 (2009) 083519.

[14] K. Orita, M. Kawaguchi, Y. Kawaguchi, S. Takigawa, D. Ueda, Efficient outdiffusion of hydrogen from Mg-doped nitrides by NF_3 annealing. J. Electron. Mater. 38 (2009) 538.

[15] D.C. Messina, K.A. Hatch, S. Vishwakarma, D.J. Smith, Y. Zhao, R.J. Nemanich, Challenges in atomic layer etching of gallium nitride using surface oxidation and ligand-exchange, J. Vac. Sci. Technol. A 41 (2023) 022603.

[16] T. Yayama, T. Chikyow, Defect control with fluorine for GaN-MIS type electronic devices. in 77th JSAP Autumn Meet. (2016).

[17] V. M. Bermudez, Investigation of the initial chemisorption and reaction of fluorine (XeF_2) with the GaN(0001)-(1 × 1) surface. Appl. Surf. Sci. 119 (1997) 147.

[18] D.D. Wagman, W.H. Evans, V.B. Parker, R.H. Schumm, I. Halow, The NBS tables of chemical thermodynamic properties: selected values for inorganic and C1 and C2 organic substances in SI units (National Bureau of Standards, 1982).

[19] N.N. Greenwood, A. Earnshaw, Chemistry of the Elements, 2nd ed (Butterworth-Heinemann, Oxford ; Boston, 1997).

[20] A. Kennedy, C.B. Colburn, Strength of the N–F bonds in NF_3 and of N–F and N–N bonds in N_2F_4. J. Chem. Phys. 35 (1961) 1892.

[21] C.J. Powell, A. Jablonski, I.S. Tilinin, S. Tanuma, D.R. Penne, Surface sensitivity of Auger-electron spectroscopy and X-ray photoelectron spectroscopy. J. Elec. Spec. Relat. Phenom. 98-99 (1999) 1.

[22] S. Ueda, M. Tanaka, H. Yoshikawa, Y. Yamashita, Y. Matsushita, K. Kobayashi, Present

status of the NIMS contract beamline BL15XU at SPring-8. AIP Conf. Proc. 1234 (2010) 403.

[23] S. Ueda, Application of hard X-ray photoelectron spectroscopy to electronic structure measurements for various functional materials. J. Electron Spectrosc. Rel. Phenom. 190, (2013) 235.

[24] J. Libra, KolXPD (Kolibrik.net).

[25] A. Thorne, U. Litzén, S. Johansson, Spectrophysics: Principles and Applications (Springer Science & Business Media, 1999).

[26] D.A. Shirley, High-Resolution X-Ray photoemission spectrum of the valence bands of gold. Phys. Rev. B, 5 (1972) 4709.

[27] S. Doniach, M. Šunjić, Many-electron singularity in X-ray photoemission and X-ray line spectra from metals. J. Phys. C Solid State Phys. 3 (1970) 285.

[28] J.F. Moulder, W.F. Stickle, P.E. Sobol, K.D. Bomben, Handbook of X-Ray Photoelectron Spectroscopy (Perkin-Elmer, Eden Prairie, MN, USA, 1992).

[29] NIST X-Ray Photoelectron Spectroscopy Database, NIST Standard Reference Database Number 20, Version 4.1 (National Institute of Standards and Technology, 2012).

[30] Y. Youngrak Park, J. Kim, W. Chang, D. Jung, S. Bae, J. Mun, C.-H. Jun, S. Ko, E. Nam, Normally-off GaN MIS-HEMT using a combination of recessed-gate structure and CF_4 plasma treatment. Phys. Status Solidi A, 212 (2015) 1170.

[31] L.R. Williston, I. Bello, W.M. Lau, X-ray photoelectron spectroscopic study of the interactions of fluorine ions with gallium arsenide. J. Vac. Sci. Technol. A, 10 (1992) 1365.

[32] P.R. Varekamp, W.C. Simpson, D.K. Shuh, T.D. Durbin, V. Chakarian, J.A. Yarmoff, Electronic structure of GaF_3 films grown on GaAs via exposure to XeF_2. Phys. Rev. B, 50 (1994) 14267.

[33] W.C. Simpson, P.R. Varekamp, D.K. Shuh, J.A. Yarmoff, Soft x-ray photoelectron spectroscopy study of the reaction of XeF_2 with GaAs. J. Vac. Sci. Technol. A, 13 (1995) 1709.

[34] W.C. Simpson, P.R. Varekamp, D.K. Shuh, J.A. Yarmoff, The growth of GaF_3 films on GaAs(l10) at elevated temperatures studied with soft x-ray photoelectron spectroscopy. J. Appl. Phys. 77 (1995) 2751.

[35] T.D. Veal, P.H. Jefferson, L.F.J. Piper, C.F. McConville, T.B. Joyce, P.R. Chalker, L. Considine, H. Lu, W.J. Schaff, Transition from electron accumulation to depletion at InGaN surfaces. Appl. Phys. Lett. 89 (2006) 202110.

[36] G. Martin, S. Strite, A. Botchkarev, A. Agarwal, A. Rockett, H. Morkoç, W.R.L. Lambrecht, B. Segall, Valence-band discontinuities of wurtzite GaN, AlN, and InN heterojunctions measured by x-ray photoemission spectroscopy. Appl. Phys. Lett. 65 (1994) 610.

[37] T. Ohsawa, S. Ueda, M. Suzuki, Y. Tateyama, J.R. Williams, N. Ohashi, Investigating crystalline-polarity-dependent electronic structures of GaN by hard x-ray photoemission and ab-initio calculations. Appl. Phys. Lett. 107 (2015) 171604.

[38] F. Liu, R. Collazo, S. Mita, Z. Sitar, G. Duscher, S.J. Pennycook, The mechanism for polarity inversion of GaN via a thin AlN layer: Direct experimental evidence. Appl. Phys. Lett. 91 (2007) 203115.

[39] R.M. Feenstra, J.E. Northrup, J. Neugebauer, Review of structure of bare and adsorbate-covered GaN(0001) surfaces. MRS Internet J. Nitride Semicond. Res. 7, (2002) 1.

[40] S. Tanuma, C.J. Powell, D.R. Penn, Calculations of electron inelastic mean free paths. V. Data for 14 organic compounds over the 50-2000 eV range. Surf. Interface Anal. 21 (1994) 165.

[41] M. Grabau, S.K. Calderón, F. Rietzler, I. Niedermaier, N. Taccardi, P. Wasserscheid, F. Maier, H-P. Steinrück, C. Papp, Surface enrichment of Pt in Ga_2O_3 films grown on liquid Pt/Ga alloys. Surf. Scie. 651 (2016) 16.

[42] F. P. Gortsema and R. H. Toeniskoetter, The Chemistry of Platinum Hexafluoride. I. Reactions with Nitric Oxide, Dinitrogen Tetroxide, Nitrosyl Fluoride, and Nitryl Fluoride. Inorg. Chem. 5 (1966) 1217.

[43] A. Kotsifa, D.I. Kondarides, X.E. Verykios, Comparative study of the chemisorptive and

catalytic properties of supported Pt catalysts related to the selective catalytic reduction of NO by propylene. Appl. Catal. B: Environ. 72 (2007) 136

Supplementary data

NF_3 and F_2 Gas Fluorination of GaN Surface and Pt/GaN Interface Analyzed by Hard X-ray Photoelectron Spectroscopy

Asahiko Matsuda[a], Takashi Teramoto[b], Takahiro Nagata[c,*], Dominic Gerlach[c,1], Peng Shen[b], Shigenori Ueda[c,d], Takako Kimura[b], Christian Dussarrat[b], and Toyohiro Chikyow[e]

[a] Materials Data Platform, National Institute for Materials Science (NIMS), 1-1 Namiki, Tsukuba, Ibaraki 305-0044, Japan

[b] K.K. Air Liquide Laboratories, 2-2 Hikarinooka, Yokosuka, Kanagawa, 239-0847, Japan

[c] Research Center for Electronic and Optical Materials, NIMS, 1-1 Namiki, Tsukuba, Ibaraki 305-0044, Japan

[d] Synchrotron X-ray Station at SPring-8, NIMS, Sayo, Hyogo 679-5148, Japan

[e] Center for Basic Research on Materials, NIMS, 1-1 Namiki, Tsukuba, Ibaraki 305-0044, Japan

* Correspondence to: NAGATA.Takahiro@nims.go.jp

[1] Current affiliation; Zernike Institute for Advanced Materials, University of Groningen Nijenborgh 4, 9747 AG Groningen, The Netherlands

[Sample preparation]

Figure S1 shows a schematic of the sample preparation process. Samples were annealed at 500°C for 120 s in either an NF_3 or F_2. One group of samples did not undergo Pt deposition. Two other groups of samples had a layer of Pt deposited either after or before the gas annealing.

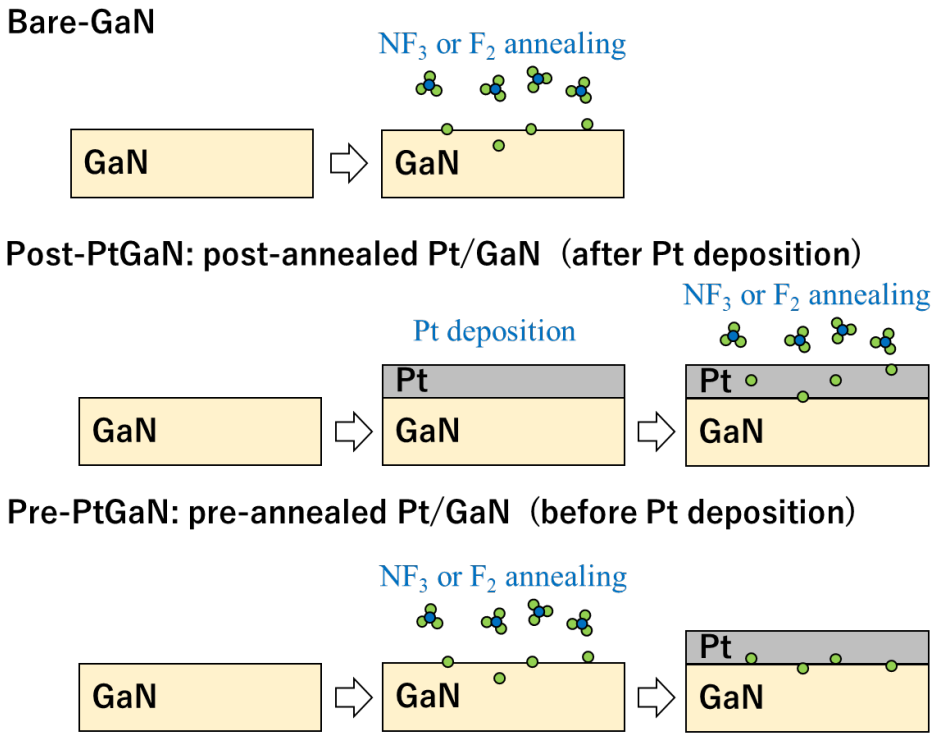

Figure S1. Schematics of the sample preparation and gas treatment processes.

[Valence-band spectrum]

The entire structure of valence band and Ga 3*d* spectra were shown in Fig. S2. The NF_3-treated sample shows an additional peak around 23 eV corresponding to GaF_x and a peak shift to E_F.

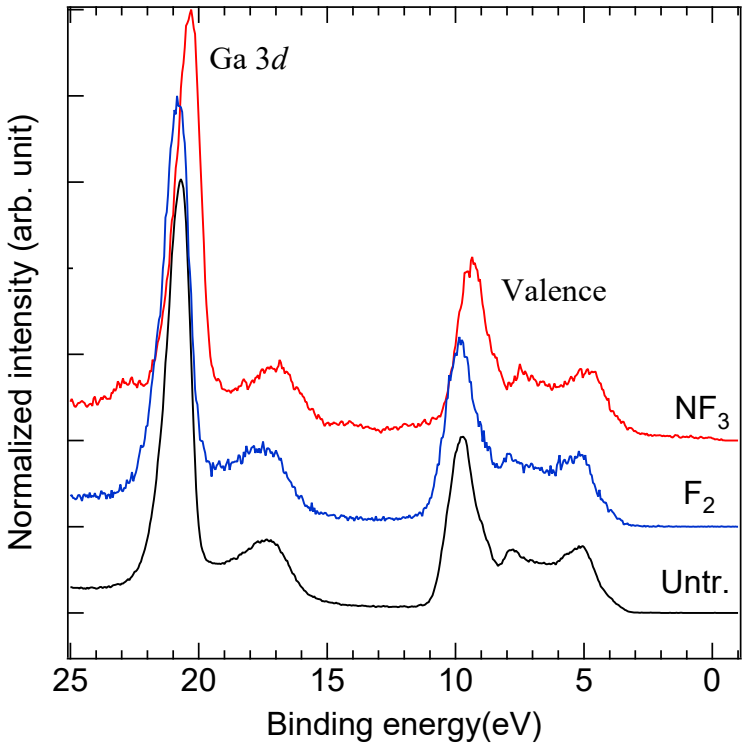

Figure S2. Valence-band and Ga 3*d* spectra for NF_3-treated, F_2-treated, and untreated Bare-GaN.

[Schottky properties]

For the electrical properties on the NF_3 treated Post- and Untreated PtGaN, a vertical device structure with top and bottom electrodes formed on GaN bulk crystals (Shinyo co. ltd., thickness: 362 μm) was used to simplify the sample fabrication process and to suppress the effect of surface modification by the additional wet process.

For electrical measurements, a Pt top electrode with a diameter of 110 μm and a thickness of 250 nm was formed by DC-sputtering with a metal mask. On the back side, a 12 nm thick Ti/100 nm thick Pt stacked ohmic electrode was formed by DC-sputtering. Some of the samples were treated with NF_3. Current-voltage (I-V) measurements were performed using a semiconductor parameter analyzer (Keysight Technologies, B1500A). To investigate the Schottky barrier height in detail, the I-V characteristics were analyzed using the theoretical equation of thermal electron emission (S. M. Sze, Physics of Semiconductors Devices Wiley, New York, 1981., A. Kumar, *et al.*, Nano. Res. Lett. 8 (2013) 481.).

Figure S3 shows I-V properties of NF_3-treated and Untreated Pt-GaN. The values of Φ_B of NF_3-treated and untreated samples are obtained as 1.09 and 0.92 eV, and their ideality factors are also estimated as 1.22 and 1.22, respectively.

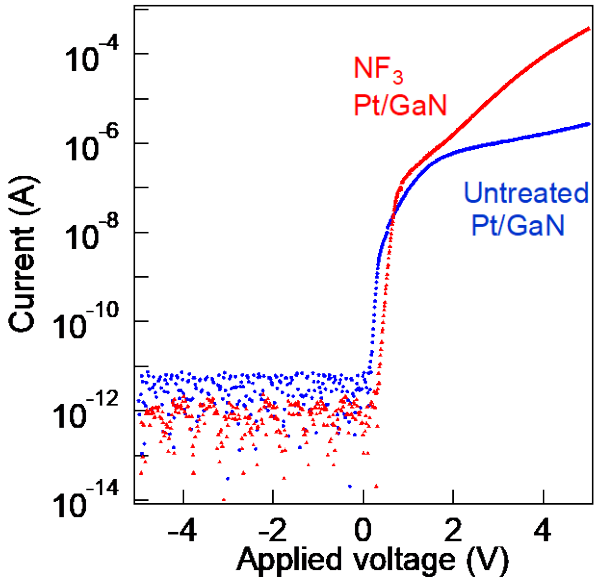

Figure S3. I-V properties of NF_3-treated and Untreated Pt-GaN.

[Summary of the results]

The effects of NF_3 treatment are observed not only in bare GaN samples but also in Pt/GaN samples treated with NF_3 after Pt deposition; however, they are not observed for Pt/GaN samples treated with NF_3 before Pt deposition.

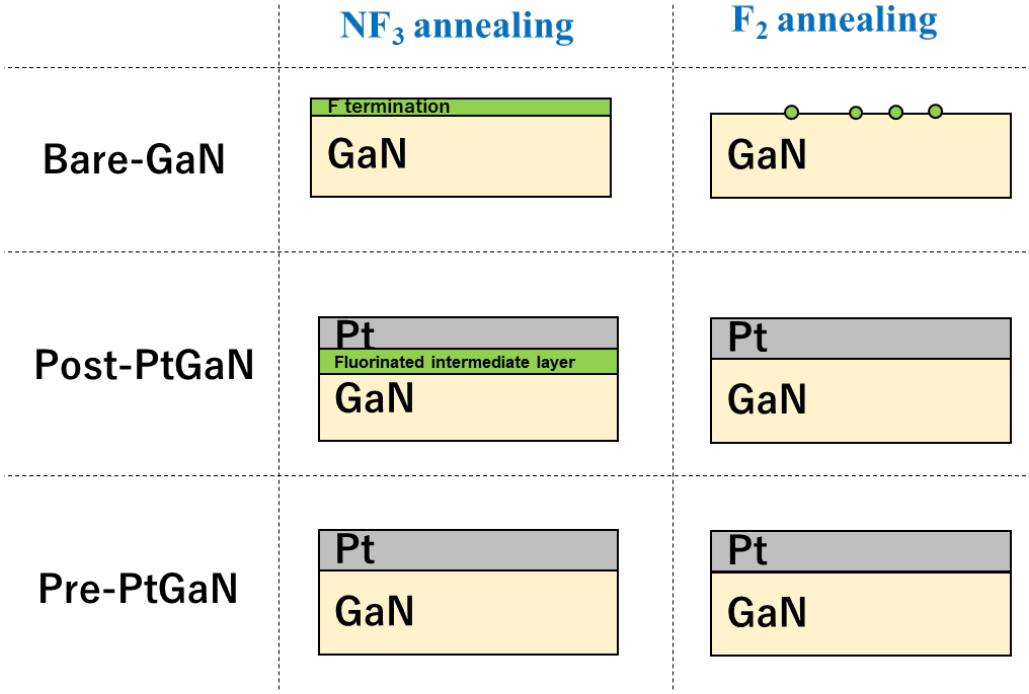

Figure S4. Illustration of the effects of fluorine-containing gas treatment on GaN surfaces.